photonics

IMPACT FACTOR 2.536

CITESCORE 2.3

Article

Implementation of Photonic Phase Gate and Squeezed States via a Two-Level Atom and Bimodal Cavity

Shiqing Tang, Xi Jiang, Xinwen Wang and Xingdong Zhao

Special Issue

Quantum Optics: Science and Applications

Edited by

Dr. Hua-Lei Yin, Dr. Peng Xu and Dr. Jie Chen

MDPI

https://doi.org/10.3390/photonics9080583

photonics

MDPI

Article

Implementation of Photonic Phase Gate and Squeezed States via a Two-Level Atom and Bimodal Cavity

Shiqing Tang [1,2], Xi Jiang [1], Xinwen Wang [1,2,*] and Xingdong Zhao [3]

[1] College of Physics and Electronic Engineering, Hengyang Normal University, Hengyang 421002, China
[2] Key Laboratory of Low-Dimensional Quantum Structures and Quantum Control of Ministry of Education, Hunan Normal University, Changsha 410081, China
[3] School of Physics, Henan Normal University, Xinxiang 453000, China
* Correspondence: xwwang@hynu.edu.cn

Abstract: We propose a theoretical model for realizing a photonic two-qubit phase gate in cavity QED using a one-step process. The fidelity and probability of success of the conditional quantum phase gate is very high in the presence of cavity decay. Our scheme only employs one two-level atom, and thus is much simpler than other schemes involving multi-level atoms. This proposal can also be applied to generate two-mode squeezed states; therefore, we give three examples, i.e., the two-mode squeezed vacuum state, two-mode squeezed odd coherent state, and two-mode squeezed even coherent state, to estimate the variance of Duan's criterion when taking into account cavity decay. It is shown that the variance is smaller than 2 for the three squeezed states in most cases. Furthermore, we utilize logarithmic negativity to measure the entanglement, and find that these squeezed states have very high degrees of entanglement.

Keywords: bimodal cavity; two-level atom; phase gate; squeezed state; one-step

Citation: Tang, S.; Jiang, X.; Wang, X.; Zhao, X. Implementation of Photonic Phase Gate and Squeezed States via a Two-Level Atom and Bimodal Cavity. *Photonics* **2022**, *9*, 583. https://doi.org/10.3390/photonics9080583

Received: 4 August 2022
Accepted: 15 August 2022
Published: 18 August 2022

1. Introduction

The process of quantum information processing is a series of unitary evolutions of quantum states encoded as quantum information. A quantum logic gate is a kind of unitary transformation that operates on qubits, which can control and manipulate the evolution of quantum states. It can be represented by the unitary operator U, i.e., it evolves one quantum state into another. Thus, the input quantum states and the output quantum states are related by the unitary evolution operator U. The manipulation of quantum states is achieved by the rational construction of the evolution matrix U. According to the requirements of the quantum algorithm, the unitary transformation called "quantum logic gate operation" is a manually controlled quantum physical evolution process with the input state as the initial state. The time evolution of quantum states is determined by the Schrödinger equation of quantum mechanics. Therefore, people naturally think it a feasible way of realizing the desired quantum logic gate by finding an appropriate Hamiltonian, so that the system evolves to the desired quantum state by a specific unitary transformation.

It is well known that universal quantum computation can be achieved by cascading quantum phase gates and single-qubit gates, since any unitary transformation can be decomposed into these elementary gates. Controlled phase gates play an important role in quantum information processing [1–4]. The effect of the two-qubit controlled phase gate causes the phase to flip when two qubits are in the target state [5,6]. Various theoretical schemes have been proposed to realize controlled phase gates based on cavity QED technology [7–16]. According to different information carriers, these phase gates can be divided into three categories. The first category encodes quantum information in atoms by using dynamic evolution or adiabatic evolution, with which two-qubit phase gates can be implemented. Meanwhile, excellent schemes have also been proposed to realize controlled phase gates of N ofqubits [1–5]. The second category is hybrid encoding, where

quantum information is encoded in both cavity fields and atoms. This type of two-qubit controlled phase gate can be realized by a Raman transition and subsequently generalized to a three-qubit controlled phase gate (encoded by two cavity fields and an atom) [4]. The third category encodes quantum information in two nondegenerate cavity fields [17–22]. Solano proposed a scheme to realize this kind of controlled phase gate using Ξ-position atoms, but this scheme ignores the Stark shift term of the whole system Hamiltonian [18]. Recently, gate operations have been realized in *V*-type [20], Λ-type [21] and Ξ-type [22] atoms by precisely choosing the interaction time and the amount of frequency detuning between the single atom and the cavity field [23,24].

It is well known that the quantum states are the carrier of quantum information, and quantum information processing [25–30] is the manipulation of quantum states in the final analysis. Therefore, many methods for preparing quantum states have been proposed [31–40]. For example, two-mode squeezed states are of crucial importance for quantum communication [41] and nonlocality tests [42] with continuous variable states. Recently, entangled squeezed states of two electromagnetic field modes were used for the teleportation of quantum states with continuous variables [43]. Similar to the implementation of quantum logic gates, preparation of the quantum state is performed to manipulate the transformation or evolution of the qubits in the quantum system, while controlling the evolution of the quantum qubit state is performed to find and manipulate the Hamiltonian that is able to realize the interaction between the quantum qubit and the external field, and thus the goal of the target state can achieve by adjusting the system parameters and selecting the appropriate interaction time. In particular, the squeezed vacuum state can be obtained by applying the squeezed operator on the vacuum state, and the squeezed operator is determined by the Hamiltonian of light–matter interaction.

In this paper, we construct a theoretical model, inspired by the above-mentioned works, to implement a conditional quantum phase gate operation and prepare two-mode squeezed states using one two-level atom simultaneously interacting with two-mode cavity fields. Our proposal has the following distinct advantages: (i) Our scheme only employs one two-level atom, and is thus easier to implement than the aforementioned proposals involving multi-level atoms. (ii) The scheme can also be applied to generate two-mode squeezed states with very high degrees of entanglement. (iii) The fidelity and success probability of the conditional quantum phase gate is very high in the presence of cavity dissipation.

2. The Model and Effective Hamiltonian

In the following, we will show how to engineer frequency down-conversion interaction by considering the physical model of a two-level atom interacting with two cavity modes and driven additionally by one external classical field. The character of the frequency down-conversion-type coupling between two cavity modes is that the creation of one photon in mode 1 is accompanied by the creation of one photon in mode 2, and vice versa [24]. The interaction is associated with a parametric amplifier, which can be used directly to generate a two-mode squeezed state. Our scheme is different from other schemes in two respects. First, in previous schemes, the internal state of the atom is used as one qubit, and the internal state of the cavity field is used as another qubit, but the experimental implementation of typical quantum algorithms generally requires two qubits to be in the same information carrier. In our scheme, the $|0\rangle$ and $|1\rangle$ photon states of two different polarization modes of the radiation field in the cavity are regarded as two qubits. Second, the required frequency down-conversion can be implemented by only a two-level atom interacting with the bimodal cavity, and thus is much simpler than other schemes involving multi-level atoms.

As shown in Figure 1, we consider one two-level atom simultaneously interacting with two cavity modes and driven by one classical field. The cavity modes are coupled to the transition $|g\rangle \rightarrow |e\rangle$ and g_j is the coupling strength between the atom and the j-th cavity mode ($j = 1, 2$). a_j ($a_j{}^\dagger$) is used to denote the creation (annihilation) operator of photons in the j-th cavity mode, and ω_j is utilized to describe the eigenfrequency of the corresponding cavity mode. The two-level atom also interacts with an external classical field with Rabi frequency Ω. Without cavity decay, the Hamiltonian of the system under the rotating wave approximation is described by (assuming $\hbar = 1$).

$$H = H_0 + H_I \tag{1}$$

with

$$H_0 = \frac{\omega_0}{2}(|e\rangle\langle e| - |g\rangle\langle g|) + \sum_{j=1}^{2} \omega_j a_j{}^\dagger a_j \tag{2}$$

$$H_{int} = \Omega\Big(|e\rangle\langle g|e^{-i\omega_0 t} + |g\rangle\langle e|e^{i\omega_0 t}\Big) + \sum_{j=1}^{2} g_j\Big(a_j|e\rangle\langle g| + a_j^\dagger|g\rangle\langle e|\Big) \tag{3}$$

For simplicity, we assume that g_j, ω_j and Ω are real numbers. Then, the Hamiltonian describing the atom–field interaction in the interaction picture is given by

$$H_I = \Omega(|e\rangle\langle g| + |g\rangle\langle e|) + \sum_{j=1}^{2} g_j\Big(a_j e^{-i\Delta_j t}|e\rangle\langle g| + a_j^\dagger e^{i\Delta_j t}|g\rangle\langle e|\Big) \tag{4}$$

where Δ_j is the detuning of the cavity modes with the atomic transition frequency. Introducing the new atomic basis $|+\rangle = \frac{1}{\sqrt{2}}(|g\rangle + |e\rangle)$,$|-\rangle = \frac{1}{\sqrt{2}}(|g\rangle - |e\rangle)$ [44–51], we can rewrite the Hamiltonian H_I as

$$H_I = \Omega\sigma_z + \sum_{j=1}^{2}\Big[g_j a_j e^{-i\Delta_j t}\big(\sigma_z + \sigma^+ - \sigma^-\big) + g_j a_j^\dagger e^{i\Delta_j t}\big(\sigma_z + \sigma^- - \sigma^+\big)\Big] \tag{5}$$

where $\sigma_z = |+\rangle\langle+| - |-\rangle\langle-|$, $\sigma^+ = |+\rangle\langle-|$,$\sigma^- = |-\rangle\langle+|$. Performing a unitary transformation $U = exp(-i\Omega\sigma_z t)$ on this Hamiltonian and applying the formula $H_I' = U^\dagger H_I U - i\frac{dU^\dagger}{dt}U$, we can obtain a Hamiltonian with the following form:

$$H_I' = \left[\sum_{j=1}^{2}\frac{g_j}{2}a_j e^{-i\Delta_j t}\Big(\sigma_z + e^{2i\Omega t}\sigma^+ - e^{-2i\Omega t}\sigma^-\Big)\right] + H.c. \tag{6}$$

This Hamiltonian presents fast oscillating time dependence, which allows us to apply the effective Hamiltonian approach proposed in Ref. [52] to simplify it. By setting $\Delta_1 + \delta - \Delta_2 = 0$ and $\Delta_1 \gg \delta$, we can neglect the term δ in the denominator. Considering the large detuning limit, i.e., $\Delta \sim \Omega \gg g_1$,$g_2$ and $2\Omega + \Delta_1 \gg 2\Omega - \Delta_1$, these terms like $\frac{g_1 a_1}{\Delta_1}$, $\frac{g_1 a_1}{2\Omega+\Delta}$, etc., can be ignored. At the same time, under the condition of the rotating wave approximation, the high frequency rapid oscillating terms can be neglected [44–48]. This leads to an effective Hamiltonian with $\varepsilon = 2\Omega - \Delta_1$, $\vartheta_j = \frac{g_j^2}{4\varepsilon}$, $(j = 1, 2)$ and $\zeta = \frac{g_1 g_2}{4\varepsilon}$ as follows:

$$H_{eff} = \vartheta_1\Big(a_1^\dagger a_1\sigma_z + \sigma^+\sigma^-\Big) + \vartheta_2\Big(a_2^\dagger a_2\sigma_z + \sigma^-\sigma^+\Big) - \sigma_z\Big(\zeta e^{i\delta t}a_1 a_2 + H.c.\Big) \tag{7}$$

Here, we assume that the atom is initially in the state $|-\rangle$; then, the atomic state remains unchanged and the cavity field state is decoupled with the atomic part. To further simplify the dynamics of the system, we have to make further approximations. Performing the unitary transformation $U = exp(\sum_{j=1}^{2} -i\vartheta_j a_j^{\dagger} a_j t)$, a new Hamiltonian $H'_{eff} = U^{\dagger} H_{eff} U - i\frac{dU^{\dagger}}{dt} U$ can be obtained. Adjust the parameter appropriately $\vartheta_1 + \vartheta_2 - \delta = 0$, so that the Hamiltonian is finally simplified to [50,51]

$$H'_{eff} = \zeta a_1 a_2 + H.c. \tag{8}$$

This is a Hamiltonian of frequency down-conversion between two cavity modes, which has a wide range of applications in quantum optics and quantum information.

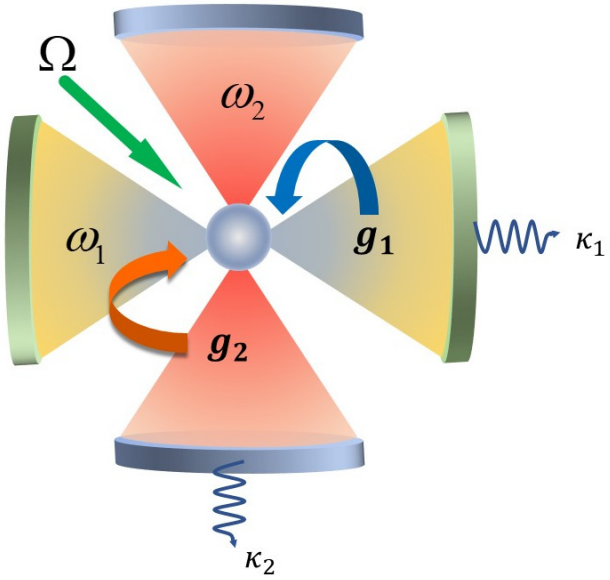

Figure 1. Experimental setup. One atom is localized in the optical cavity, with one two-level atom simultaneously interacting with two cavity modes (ω_1, ω_2) and driven by one classical field (Ω); κ_1 and κ_2 are the cavity decay coefficients.

3. Two-Qubit Phase Gate and Fidelity Analysis

We can now consider how to realize a two-qubit photonic phase gate. Our scheme uses cavity fields as the quantum memory, and quantum information is transferred directly in the cavity modes. Let us substitute the effective Hamiltonian of the system into the Schrödinger equation:

$$i\frac{\partial}{\partial t}|\Psi(t)> = H'_{eff}|\Psi(t)> \tag{9}$$

We assume that the computational basis states are encoded on vacuum and single-photon states $\{|0_1, 0_2\rangle, |0_1, 1_2\rangle, |1_1, 0_2\rangle, |1_1, 1_2\rangle\}$. It is obvious that once one cavity mode is initially in the vacuum state, the atom–cavity system does not experience any dynamical evolution, since $H'_{eff}|0_1, \alpha_2\rangle = |0_1, \alpha_2\rangle$, ($\alpha \in 0, 1$) and $H'_{eff}|1_1, 0_2\rangle = |1_1, 0_2\rangle$. In other words, we only need to consider the temporal evolution of the initial system state $|1_1, 1_2\rangle$. After solving the Schrödinger equation, we obtain the temporal evolution:

$$\psi(t) = \cos\zeta t|1_1, 1_2\rangle - i\sin\zeta t|0_1, 0_2\rangle \tag{10}$$

when the interaction time is taken as $\zeta t = \pi$, the system returns to the target state with additional phase shift π. As a whole, we have

$$\begin{array}{c} |0_1, 0_2\rangle \rightarrow |0_1, 0_2\rangle \\ |0_1, 1_2\rangle \rightarrow |0_1, 1_2\rangle \\ |1_1, 0_2\rangle \rightarrow |1_1, 0_2\rangle \\ |1_1, 1_2\rangle \rightarrow -|1_1, 1_2\rangle \end{array} \tag{11}$$

The form of Equation (11) can be considered as a two-qubit quantum phase gate operation. This quantum gate implies that if and only if both qubits are in the state |1>, there will accumulate a global phase π. Figure 2 shows the simple procedure for a two-qubit quantum logic gate implementation process.

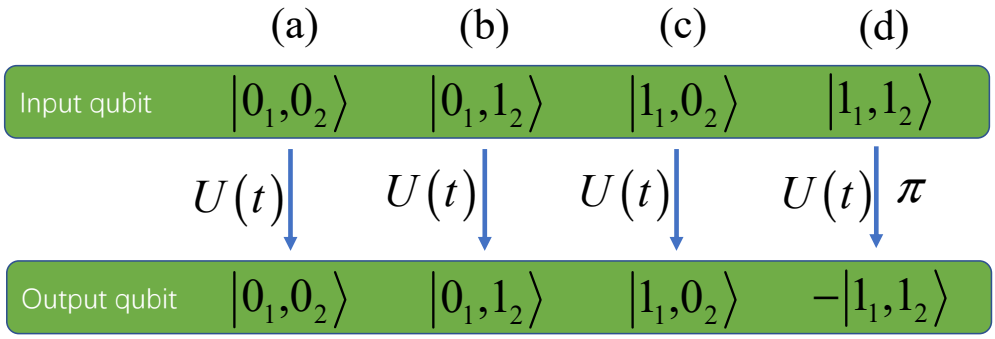

Figure 2. The procedure diagram for a two-qubit quantum logic gate protocol using effective Hamiltonian (8).

The above analysis is carried out without cavity decay. Next, we consider the decoherence effect of the system. When considering the decay of the cavity, the master equation of the system is described by $\frac{d\rho}{dt} = -i[H, \rho] + \frac{\kappa}{2}\sum_{j=1}^{2}\left(2a_j\rho a_j^\dagger - a_j^\dagger a_j\rho - \rho a_j^\dagger a_j\right)$, and $\kappa_1 = \kappa_2 = \kappa$ are the cavity decay coefficients. To check the validity of the scheme, we give the evolution of the system and the fidelity of the gate operation by using the numerical calculation. The fidelity is given by:

$$F \equiv |\langle\Psi_{out}|\Psi_{ideal}\rangle|^2 \tag{12}$$

where $|\Psi_{out}\rangle$ is the actual output state under dissipation according to the master equation, and $|\Psi_{ideal}\rangle$ is the output state of an ideal system without decay. For the initial state of the system $|\Psi_0\rangle = (|0\rangle_1 + |1\rangle_1)(|0\rangle_2 + |1\rangle_2)/2$, we plot the fidelity of the two-qubit phase gate vs. κ/ζ, as shown in Figure 3a. From that, it can be seen that the gate fidelity monotonically drops when κ/ζ grows during the gate implementation. However, the fidelity is still greater than 98% when κ/ζ is lower than 0.1. Meanwhile, cavity decay plays an important role in the dissipative channel during the gate implementation. The outcome of the numerical calculation $P = 1 - \langle\Psi_{out}|\Psi_{out}\rangle$ on the photon loss after a full gate operation is shown in Figure 3b. It can be observed that the photon loss is proportional to κ/ζ when $g_1 = g_2 = g$. In addition, the photon loss of the cavity is not serious under the condition of slight strong coupling. Figure 3b shows the probability of successful realization of a photonic two-qubit phase gate, which monotonically decreases as the decay coefficients of the cavity and atom increase.

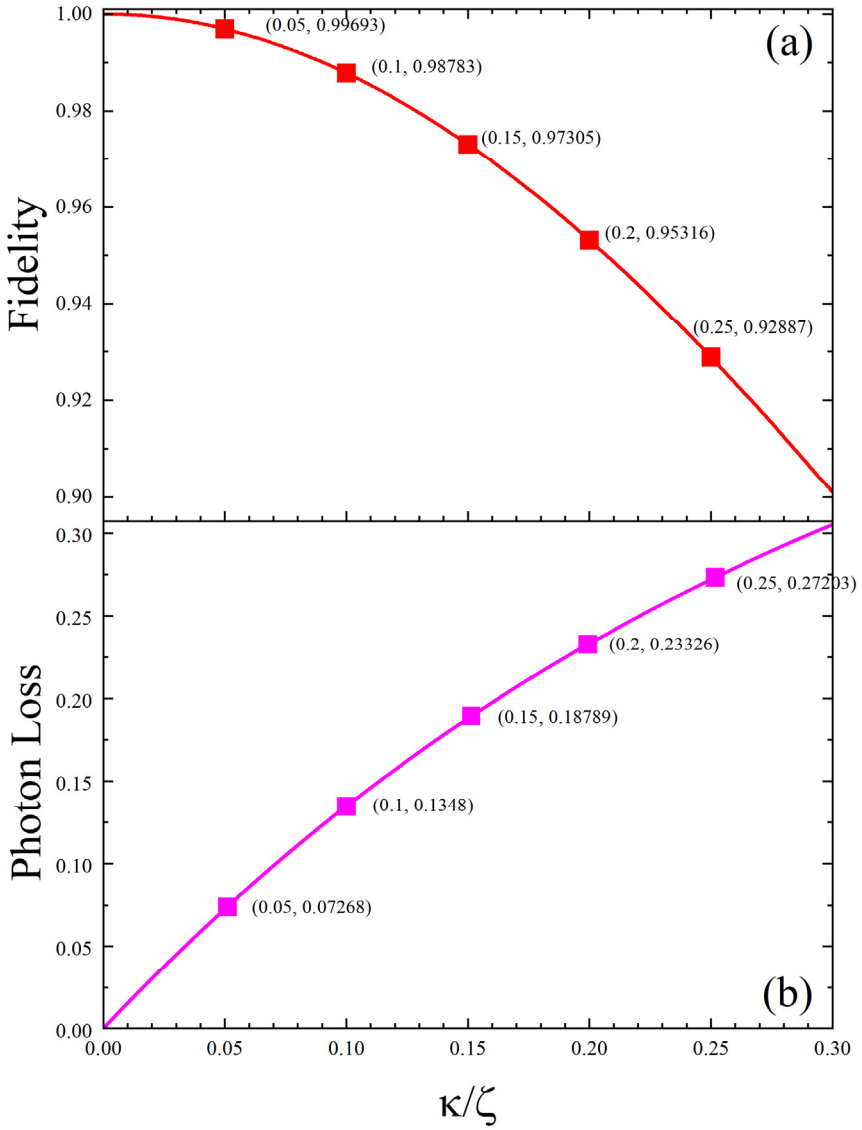

Figure 3. (**a**) Fidelity of the photonic two-qubit phase gate. (**b**) Photon loss during the implementation of the phase gate, where $\kappa_1 = \kappa_2 = \kappa$, $\zeta = \frac{g_1 g_2}{4\varepsilon}$, $g_1 = g_2 = g$, $\varepsilon = 5g$.

We now discuss the effect of some imperfections in the experiment. First, the coupling strength g in the optical cavity is not a constant in the current technique, because the coupling strength depends on the position of the atom in the cavity mode volume [21], while it is very difficult to precisely manipulate atoms in the experiment. Considering the unavoidable deviation of g by the value δ_g, that is, $g\prime = \delta_g + g$ [21], Figure 4a shows the gate fidelity as a function of δ_g/g. We can see that when δ_g is not too large, the gate fidelity can be higher than 0.99, although it decreases with increasing δ_g. Second, in order to perfectly implement the quantum phase gate, the interaction time of the atom with cavity modes must be precisely controlled. In the experiment, fluctuations of parameters will induce some imperfections in the quantum gate. Here, we resort to the master equation to estimate the fidelity when taking into account the fluctuation of the interaction time. Assuming that interaction time t has a deviation of δ_t with respect to the ideal value owing to the velocity fluctuation of the atom [23], Figure 4b plots the fidelity as a function of the parameter δ_t/t. It can be observed that under relatively small fluctuations in interaction time, the fidelity is still very close to unity. When the fluctuation in interaction time δ_t/t is smaller than 20%, the fidelity is still larger than 99.6%.

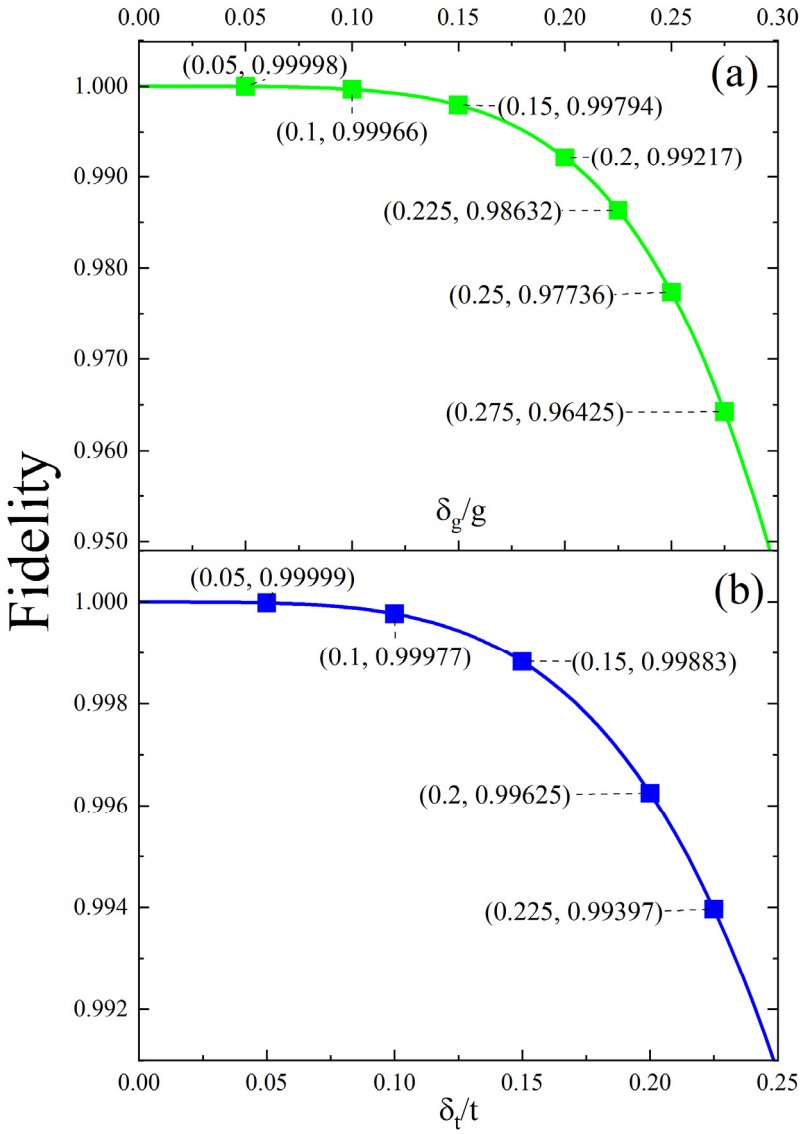

Figure 4. Fidelity of photonic two-qubit phase gate in the condition of deviation of g by the value δ_g (**a**) and deviation of t by the value δ_t (**b**), where the other parameters are chosen to be the same as those in Figure 3.

4. Generation of Two-Mode Squeezed States and Entanglement Analysis

In this section, we present an alternative scheme for the deterministic generation of two-mode squeezed states in the aforementioned bimodal cavity QED system, with resort to the effective Hamiltonian. If the atom is initially in the state $|-\rangle$, it will remain in the state $|-\rangle$, and the cavity field state is decoupled with the atomic part. In this case, the effective Hamiltonian describing the evolution of the cavity field is $H'_{eff} = (\zeta a_1 a_2 + H.c.)$. The evolution of the cavity field is given by the squeeze operator:

$$S(\varsigma) = e^{\varsigma a_1^\dagger a_2^\dagger - \varsigma^* a_1 a_2} \tag{13}$$

Where the squeezed parameter is given by $\varsigma = i\zeta t$, with t being the interaction time. It should be noted that the squeezing is produced on any initial cavity state. If the cavity field is initially in the vacuum state, the squeezed vacuum state is obtained. On the other hand, for the initial coherent state, the squeezed coherent state is produced. Therefore, we give three examples, i.e., the two-mode squeezed vacuum state, two-mode squeezed

odd coherent state, and two-mode squeezed even coherent state, to estimate the variance of Duan's criterion and apply the latest favored logarithmic negativity to analyze the entangled property.

As usual, we first introduce the two quadrature components $u = X_\alpha + P_\alpha, v = X_\alpha - P_\alpha$ with $X_\alpha = \frac{\alpha e^{-i\theta} + \alpha^+ e^{i\theta}}{\sqrt{2}}$, $P_\alpha = \frac{\alpha e^{-i\theta} - \alpha^+ e^{i\theta}}{\sqrt{2}i}$,$(\alpha = a_1, a_2)$ and build the squeezing or entanglement criterion. The parameter θ refers to the squeezing direction. This criterion for inseparability was developed by Duan et al., which provides a sufficient condition for the entanglement of any bipartite continuous-variable system. If a state is not separable, the uncertainties in a pair of EPR-like operators X_α, P_α satisfy the following equation (variance V will less than 2) [53]:

$$V = \left\langle (\Delta u)^2 + (\Delta v)^2 \right\rangle \tag{14}$$

To quantify the squeezing with experimentally attainable parameters, we perform a direct numerical calculation while taking into account the decay of the cavity modes. It has been shown that the variance V is always smaller than 2 for an entangled two-mode state [52]. In the numerical calculation, we assume that the system is initially prepared in the state $|0_1, 0_2\rangle$. In Figure 5a, the steady-state variances versus squeezed strength r are plotted, where the solid, dash-dotted, and dashed lines represent, respectively, the situations of the ideal squeezed vacuum $\kappa = 0$, $\kappa = 0.05\zeta$ and $\kappa = 0.1\zeta$. For $\kappa = 0.1\zeta$, it can be observed that the variance V deviates slightly from that of the ideal case. It has been shown that the variance V is always smaller than 2 for an entangled two-mode state.

As mentioned above, Equation (13) is a two-mode squeezed operator that can produce two-mode squeezing on any initial field state. Now, we present the following two cases to estimate the variance V for the initial state $|\psi(0)\rangle = N_\pm(|\alpha_1, \alpha_2\rangle \pm |-\alpha_1, -\alpha_2\rangle)$, where $N_\pm$ represents the normalized coefficients. It can be seen that the variance (dash-dotted line or dashed line) has almost no divergence from the ideal case (solid line) for the initial odd coherent state, as shown in Figure 5b, when taking into account the dissipation. For the initial even coherent state, it can be seen from Figure 5c that the deviation of the variance V between the decay and ideal cases increases as the decay rises. That is to say, cavity decay plays a dominant role in the dissipative channel.

Next, in order to further reveal the relationship between squeezing and entanglement, we turn to quantifying entanglement between the two modes. Because the entanglement of quantum states is a key topic in the study of quantum information, it has a great influence on the application of quantum information processing. For example, the two-mode squeezed vacuum state is a typical entangled state with continuous variables. There are many ways to measure entanglement. One common way to characterize the entanglement properties of a two-mode Gauss quantum state is to use logarithmic negativity, which is a single-valued function of the degree of entanglement. It can be expressed in a very concise way, and the calculation is greatly simplified. In particular, if the two modes are separable, the logarithmic negativity $E_N = 0$. If the two modes are in a Bell state, $E_N = 1$. For the entanglement of high dimensions, such as the entanglement of continuous variables, logarithmic negativity can be greater than 1. The logarithmic negativity E_N is defined as $E_N = max[0, -ln(2\eta)]$ as described in [54–56].

$$\eta = \frac{1}{\sqrt{2}} \sqrt{\Sigma - \sqrt{\Sigma^2 - 4\det\sigma}} \tag{15}$$

where $\Sigma = \det A + \det B - 2\det C$. Here, σ is the reduced 4×4 covariance matrix with the elements $\vec{\ell} = \{X_1, P_1, X_2, P_2\}$ and $\sigma_{mn} = \ell_m \ell_n + \ell_n \ell_m / 2$ ($m, n \in 1, 2, 3, 4$). The 2×2 matrices A, B, and C are defined according to the following matrix blocks:

$$\sigma = \begin{pmatrix} A & C \\ C^T & B \end{pmatrix} \tag{16}$$

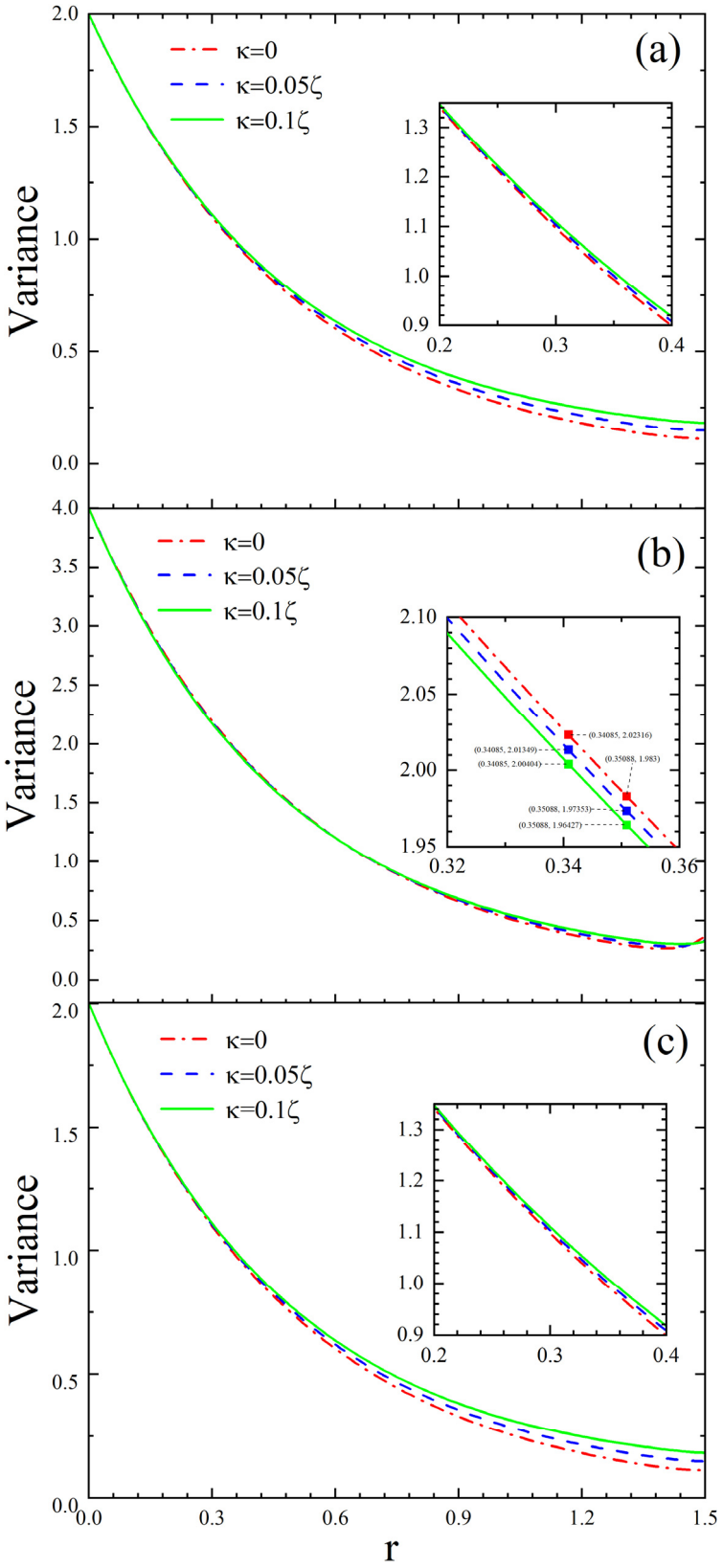

Figure 5. The total variance with different decay rates of the cavity κ versus squeezed strength r under the different initial conditions. (**a**) Initial two-mode vacuum state $|0_1, 0_2\rangle$; (**b**,**c**) initial two-mode odd/even coherent state $N_{\mp}(|\alpha_1, \alpha_2\rangle \mp |-\alpha_1, -\alpha_2\rangle)$. Here $\kappa_1 = \kappa_2 = \kappa, \zeta = \frac{g_1 g_2}{4\varepsilon}, \varepsilon = 5g$, $\alpha_1 = \alpha_2 = 0.1$.

The curves of logarithmic negativity versus squeezing coefficient for the dynamic states of the aforementioned system are displayed in Figure 6. For the squeezed vacuum state, it can be observed that the degree of entanglement increases linearly with increasing squeezing coefficient. However, for the squeezed odd coherent state, it does not exhibit entanglement properties when the squeezing coefficient is small, i.e., $r < 0.28$. After a certain degree of squeezing is reached, the entanglement begins to rise linearly with increasing squeezing coefficient. Furthermore, the logarithmic negativity of the squeezed even coherent state is the same as that of the squeezed vacuum state. From Figure 6, these three final states after the action of the two-mode squeezed operator (Equation (13)) become highly entangled states when the squeezing coefficient is greater than 1. Comparing Figures 5 and 6, it can be observed that entanglement of the three squeezed states exists in most cases. For the two-mode squeezed odd coherent state, the difference is that the logarithmic negative value is greater than 0 when $r > 0.28$, while the entanglement measured by the covariance exists only under the condition $r > 0.35$.

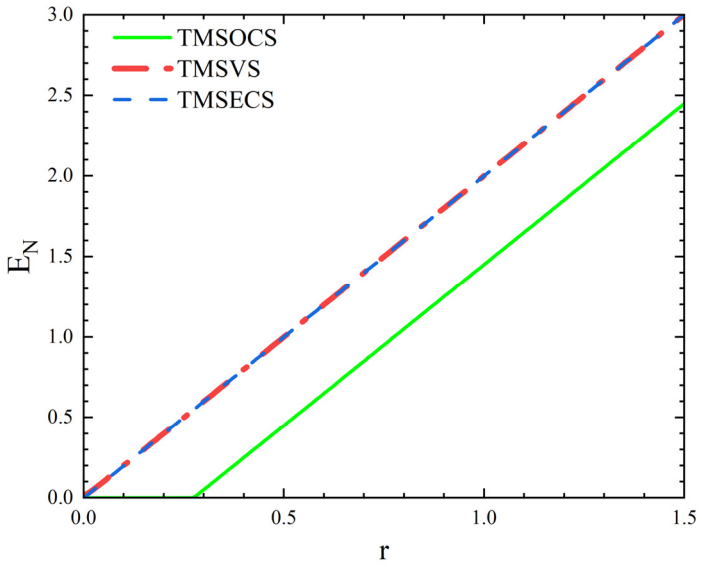

Figure 6. The logarithmic negativity of the final state for different initial states, i.e., two-mode squeezed vacuum state (TMSVS), two-mode squeezed odd coherent state (TMSOCS), two-mode squeezed even coherent state (TMSECS). Here, r denotes the squeezing strength and other parameters are chosen to be the same as those in Figures 3 and 5.

5. Conclusions

In summary, we considered a cavity QED scheme to realize a conditional quantum phase gate operation using one two-level atom simultaneously interacting with two modes of a cavity. In the scheme, a two-qubit phase gate can be implemented in one step, and the fidelity and success probability can maintain an ultrahigh level in the presence of cavity dissipation. The scheme can also be extended to realize two-mode squeezed states. The variance of Duan's criterion and logarithmic negativity showed that the generated squeezed state has a very high degree of entanglement.

Author Contributions: Conceptualization, S.T.; methodology, S.T.; software, X.J.; validation, S.T., X.J. and X.Z.; formal analysis, S.T.; investigation, S.T. and X.J.; resources, S.T.; data curation, X.J.; writing—original draft preparation, S.T.; writing—review and editing, X.W. and X.Z.; supervision, X.W. and X.Z.; project administration, S.T.; funding acquisition, S.T. All authors have read and agreed to the published version of the manuscript.

Funding: This work is supported by the Hunan Provincial Natural Science Foundation of China under Grant Nos. 2020JJ4146 and 2020JJ4002, the Open Fund project of the Key Laboratory of Optoelectronic Control and Detection Technology of University of Hunan Province under Grant No.

PC20K02, the open fund project of the Key Laboratory of Low-Dimensional Quantum Structures and Quantum Control of Ministry of Education under Grant No. QSQC1907, and the Science and Technology Plan Project of Hunan Province under Grant No. 2016TP1020.

Institutional Review Board Statement: Not applicable.

Informed Consent Statement: Not applicable.

Data Availability Statement: Not applicable.

Conflicts of Interest: The authors declare no conflict of interest.

References

1. Xiao, Y.F.; Zou, X.B.; Guo, G.C. One-step implementation of an N-qubit controlled-phase gate with neutral atoms trapped in an optical cavity. *Phys. Rev. A* **2007**, *75*, 054303. [CrossRef]
2. Zheng, S.-B. Quantum logic gates for two atoms with a single resonant interaction. *Phys. Rev. A* **2005**, *71*, 062335. [CrossRef]
3. Zheng, S.-B. Virtual-photon-induced quantum phase gates for two distant atoms trapped in separate cavities. *Appl. Phys. Lett.* **2009**, *94*, 154101. [CrossRef]
4. Tang, S.-Q.; Zhang, D.-Y.; Xie, L.J.; Zhan, X.-G.; Gao, F. Realization of three-qubit controlled-phase gate operation with atoms in cavity QED system. *Chin. Phys. Lett.* **2009**, *26*, 020310.
5. Zou, X.-B.; Xiao, Y.-F.; Li, S.-B.; Yang, Y.; Guo, G.-C. Quantum phase gate through a dispersive atom-field interaction. *Phys. Rev. A* **2007**, *75*, 064301. [CrossRef]
6. Xiao, Y.-F.; Zou, X.-B.; Han, Z.-F.; Guo, G.-C. Quantum phase gate in an optical cavity with atomic cloud. *Phys. Rev. A* **2006**, *74*, 044303. [CrossRef]
7. Asaoka, R.; Tokunaga, Y.; Kanamoto, R.; Goto, H.; Aoki, T. Requirements for fault-tolerant quantum computation with cavi-ty-QED-based atom-atom gates mediated by a photon with a finite pulse length. *Phys. Rev. A* **2021**, *104*, 043702. [CrossRef]
8. Hammani, M.; Chouikh, A.; Said, T.; Bennai, M. Realization of the quantum CNOT gate based on multiphoton process in multimode Cavity QED. *Opt. Quantum Electron.* **2021**, *53*, 89. [CrossRef]
9. Wang, Y.; Wu, J.-L.; Han, J.-X.; Jiang, Y.Y.; Xia, Y.; Song, J. Resilient Mølmer-Sørensen gate with cavity QED. *Phys. Lett. A* **2021**, *388*, 127033. [CrossRef]
10. Xu, Y.; Ma, Y.; Cai, W.; Mu, X.; Dai, W.; Wang, W.; Hu, L.; Li, X.; Han, J.; Wang, H.; et al. Demonstration of Controlled-Phase Gates between Two Error-Correctable Photonic Qubits. *Phys. Rev. Lett.* **2020**, *124*, 120501. [CrossRef]
11. Shi, Z.-C.; Zhang, C.; Shen, L.-T.; Xia, Y.; Yi, X.X.; Zheng, S.-B. Implementation of universal quantum gates by periodic two-step modulation in a weakly nonlinear qubit. *Phys. Rev. A* **2020**, *101*, 042314. [CrossRef]
12. Borne, A.; Northup, T.E.; Blatt, R.; Dayan, B. Efficient ion-photon qubit SWAP gate in realistic ion cavity-QED systems without strong coupling. *Opt. Express* **2020**, *28*, 11822–11839. [CrossRef] [PubMed]
13. Alqahtani, M.M. Multiphoton process in cavity QED photons for implementing a three-qubit quantum gate operation. *Quantum Inf. Process.* **2019**, *19*, 12. [CrossRef]
14. Devi, A.; Gunapala, S.D.; Premaratne, M. Coherent and incoherent laser pump on a five-level atom in a strongly coupled cavity-QED system. *Phys. Rev. A* **2022**, *105*, 013701. [CrossRef]
15. Alqahtani, M.M. Quantum phase gate based on multiphoton process in multimode cavity QED. *Quantum Inf. Process.* **2018**, *17*, 211. [CrossRef]
16. Chouikh, A.; Said, T.; Essammouni, K.; Bennai, M. Implementation of universal two- and three-qubit quantum gates in a cavity QED. *Opt. Quantum Electron.* **2016**, *48*, 463. [CrossRef]
17. Chang, J.-T.; Zubairy, M.S. Three-qubit phase gate based on cavity quantum electrodynamics. *Phys. Rev. A* **2008**, *77*, 012329. [CrossRef]
18. Solano, E.; Santos, M.F.; Milman, P. Quantum phase gate with a selective interaction. *Phys. Rev. A* **2001**, *64*, 024304. [CrossRef]
19. Zubairy, M.S.; Kim, M.; Scully, M.O. Cavity-QED-based quantum phase gate. *Phys. Rev. A* **2003**, *68*, 033820. [CrossRef]
20. García-Maraver, R.; Corbalán, R.; Eckert, K.; Rebić, S.; Artoni, M.; Mompart, J. Cavity QED quantum phase gates for a single longitudinal mode of the intracavity field. *Phys. Rev. A* **2004**, *70*, 062324. [CrossRef]
21. Shu, J.; Zou, X.-B.; Xiao, Y.-F.; Guo, G.-C. Quantum phase gate of photonic qubits in a cavity QED system. *Phys. Rev. A* **2007**, *75*, 044302. [CrossRef]
22. Cai, J.-W.; Fang, M.-F.; Zheng, X.-J.; Liao, X.-P. A scheme for a conditional quantum phase gate using a bimodal cavity and a ladder-type three-level atom. *J. Mod. Opt.* **2006**, *53*, 2803–2810. [CrossRef]
23. Li, P.; Gu, Y.; Gong, Q.; Guo, G. Generation of two-mode entanglement between separated cavities. *J. Opt. Soc. Am. B* **2008**, *26*, 189–193. [CrossRef]
24. Shao, X.-Q.; Chen, L.; Zhang, S. One-step implementation of a swap gate with coherent-state qubits via atomic ensemble large detuning interaction with two-mode cavity quantum electrodynamics. *J. Phys. B At. Mol. Opt. Phys.* **2008**, *41*, 245502. [CrossRef]
25. Shao, X.-Q.; Zhu, A.-D.; Zhang, S.; Chung, J.-S.; Yeon, K.-H. Efficient scheme for implementing anN-qubit Toffoli gate by a single resonant interaction with cavity quantum electrodynamics. *Phys. Rev. A* **2007**, *75*, 034307. [CrossRef]

26. Su, S.L.; Shen, H.Z.; Liang, E.; Zhang, S. One-step construction of the multiple-qubit Rydberg controlled-phase gate. *Phys. Rev. A* **2018**, *98*, 032306. [CrossRef]
27. Su, S.-L.; Gao, Y.; Liang, E.; Zhang, S. Fast Rydberg antiblockade regime and its applications in quantum logic gates. *Phys. Rev. A* **2017**, *95*, 022319. [CrossRef]
28. Su, S.L.; Liang, E.; Zhang, S.; Wen, J.J.; Sun, L.L.; Jin, Z.; Zhu, A.D. One-step implementation of the Ry-dberg-Rydberg-interaction gate. *Phys. Rev. A* **2016**, *93*, 012306. [CrossRef]
29. Kang, Y.-H.; Shi, Z.-C.; Song, J.; Xia, Y. Heralded atomic nonadiabatic holonomic quantum computation with Rydberg blockade. *Phys. Rev. A* **2020**, *102*, 022617. [CrossRef]
30. Kang, Y.-H.; Shi, Z.-C.; Huang, B.-H.; Song, J.; Xia, Y. Flexible scheme for the implementation of nonadiabatic geometric quantum computation. *Phys. Rev. A* **2020**, *101*, 032322. [CrossRef]
31. Su, S.-L.; Guo, F.-Q.; Tian, L.; Zhu, X.-Y.; Yan, L.-L.; Liang, E.-J.; Feng, M. Nondestructive Rydberg parity meter and its applications. *Phys. Rev. A* **2020**, *101*, 012347. [CrossRef]
32. Zheng, R.-H.; Kang, Y.-H.; Su, S.-L.; Song, J.; Xia, Y. Robust and high-fidelity nondestructive Rydberg parity meter. *Phys. Rev. A* **2020**, *102*, 012609. [CrossRef]
33. Zheng, R.-H.; Xiao, Y.; Su, S.-L.; Chen, Y.-H.; Shi, Z.-C.; Song, J.; Xia, Y.; Zheng, S.-B. Fast and dephasing-tolerant preparation of steady Knill-Laflamme-Milburn states via dissipative Rydberg pumping. *Phys. Rev. A* **2021**, *103*, 052402. [CrossRef]
34. Li, D.X.; Shao, X.Q. Directional quantum state transfer in a dissipative Rydberg-atom-cavity system. *Phys. Rev. A* **2019**, *99*, 032348. [CrossRef]
35. Li, D.-X.; Shao, X.; Wu, J.-H.; Yi, X.X. Dissipation-induced W state in a Rydberg-atom-cavity system. *Opt. Lett.* **2018**, *43*, 1639–1642. [CrossRef]
36. Li, D.-X.; Shao, X.; Wu, J.-H.; Yi, X.X. Engineering steady-state entanglement via dissipation and quantum Zeno dynamics in an optical cavity. *Opt. Lett.* **2017**, *42*, 3904–3907. [CrossRef]
37. Kang, Y.H.; Shi, Z.-C.; Song, J.; Xia, Y. Effective discrimination of chiral molecules in optical cavity. *Opt. Lett.* **2020**, *45*, 4952–4955. [CrossRef]
38. Guo, Y.; Shu, C.-C.; Dong, D.; Nori, F. Vanishing and Revival of Resonance Raman Scattering. *Phys. Rev. Lett.* **2019**, *123*, 223202. [CrossRef]
39. Guo, Y.; Luo, X.; Ma, S.; Shu, C.-C. All-optical generation of quantum entangled states with strictly constrained ultrafast laser pulses. *Phys. Rev. A* **2019**, *100*, 023409. [CrossRef]
40. Ma, S.; Xue, S.; Guo, Y.; Shu, C.-C. Numerical detection of Gaussian entanglement and its application to the identification of bound entangled Gaussian states. *Quantum Inf. Process.* **2020**, *19*, 225. [CrossRef]
41. Braunstein, S.L.; van Loock, P. Quantum information with continuous variables. *Rev. Mod. Phys.* **2005**, *77*, 513–577. [CrossRef]
42. Jeong, H.; Son, W.; Kim, M.S.; Ahn, D. Quantum nonlocality test for continuous-variable states with dichotomic observables. *Phys. Rev. A* **2003**, *67*, 012106. [CrossRef]
43. Furusawa, A.; Sørensen, J.L.; Braunstein, S.L.; Fuchs, C.A.; Kimble, H.J.; Polzik, E.S. Unconditional Quantum Teleportation. *Science* **1998**, *282*, 706–709. [CrossRef]
44. Li, B.; Feng, X.L.; Zhang, Z.M. Frequency Up-and Down-conversions in Two-mode Cavity. *Acta Photon. Sin.* **2011**, *40*, 1161–1165.
45. Prado, F.O.; Luiz, F.S.; Villas-Bôas, J.M.; Alcalde, A.; Duzzioni, E.I.; Sanz, L. Atom-mediated effective interactions between modes of a bimodal cavity. *Phys. Rev. A* **2011**, *84*, 053839. [CrossRef]
46. Werlang, T.; Guzmán, R.; Prado, F.O.; Villas-Bôas, C.J. Generation of decoherence-free displaced squeezed states of radiation fields and a squeezed reservoir for atoms in cavity QED. *Phys. Rev. A* **2008**, *78*, 033820. [CrossRef]
47. Zou, X.; Dong, Y.; Guo, G. Schemes for realizing frequency up- and down-conversions in two-mode cavity QED. *Phys. Rev. A* **2006**, *73*, 025802. [CrossRef]
48. Gong, W.L.; Xu, B.Z.; Ye, M.Y. Quantum SWAP gate in an optical cavity with an atomic cloud. *Phys. Rev. A* **2008**, *77*, 064301.
49. Mu, Q.-X.; Ma, Y.-H.; Zhou, L. Generation of two-mode entangled coherent states via a cavity QED system. *J. Phys. A Math. Theor.* **2009**, *42*, 225304. [CrossRef]
50. Prado, F.O.; de Almeida, N.G.; Moussa, M.H.Y.; Villas-Bôas, C.J. Bilinear and quadratic Hamiltonians in two-mode cavity quantum electrodynamics. *Phys. Rev. A* **2006**, *73*, 043803. [CrossRef]
51. Diniz, E.C.; Rossatto, D.Z.; Villas-Boas, C.J. Two-mode squeezing operator in circuit QED. *Quantum Inf. Process.* **2018**, *17*, 202. [CrossRef]
52. James, D.F.; Jerke, J. Effective Hamiltonian theory and its applications in quantum information. *Can. J. Phys.* **2007**, *85*, 625–632. [CrossRef]
53. Duan, L.-M.; Giedke, G.; Cirac, J.I.; Zoller, P. Inseparability Criterion for Continuous Variable Systems. *Phys. Rev. Lett.* **2000**, *84*, 2722–2725. [CrossRef] [PubMed]
54. Ma, S.-L.; Li, Z.; Fang, A.-P.; Li, P.; Gao, S.-Y.; Li, F.-L. Controllable generation of two-mode-entangled states in two-resonator circuit QED with a single gap-tunable superconducting qubit. *Phys. Rev. A* **2014**, *90*, 062342. [CrossRef]
55. Ma, S.-L.; Li, X.-K.; Xie, J.-K.; Li, F.-L. Two-mode squeezed states of two separated nitrogen-vacancy-center ensembles coupled via dissipative photons of superconducting resonators. *Phys. Rev. A* **2019**, *99*, 012325. [CrossRef]
56. Yang, Z.-B.; Liu, X.-D.; Yin, X.-Y.; Ming, Y.; Liu, H.-Y.; Yang, R.-C. Controlling Stationary One-Way Quantum Steering in Cavity Magnonics. *Phys. Rev. Appl.* **2021**, *15*, 024042. [CrossRef]